Electronic Supplemental information for: Insights into Pyrocumulus Aerosol Composition: Black Carbon Content and Organic Vapor Condensation

Authors: Kyle Gorkowski,[a] Eunmo Koo,[b] Spencer Jordan,[a,c] Jon Reisner,[b] Katherine B. Benedict,[a] and Manvendra Dubey[a]

1 Overview

The supplemental information contains details on the data from the flight campaigns and the organic aerosol (OA) gas-to-particle partitioning parameterization.

2 Aircraft Data

2.1 DOE-ARM Data

The aircraft data used in this study were collected from four DOE-ARM campaigns: Biomass Burning Observation Period (BBOP)[1], Carbonaceous Aerosol and Radiative Effects Study (CARES)[2], Two Column Aerosol Project (TCAP)[3], and The Cloud, Aerosol, and Complex Terrain Interactions (CACTI)[4]. These data were accessed from the DOE-ARM database, available at https://adc.arm.gov/discovery.

Black carbon (BC) measurements using the SP2 were conducted by Arthur Sedlacek (Brookhaven National Lab, sedlacek@bnl.gov). The instrument was calibrated with fullerene soot of variable mobility density. No correction was applied for the organic carbon (OC) content in the fullerene, which is estimated to be around 20% based on the sensitivity of the measurement to different types of black carbon. The Ultra-High Sensitivity Aerosol Spectrometer was operated by Jason Tomlinson (Pacific Northwest National Lab, jason.tomlinson@pnnl.gov). The instrument was calibrated in the field using polystyrene latex spheres and measured aerosol particles in the size range of 0.060 nm to 1000 nm. Carbon monoxide (CO) measurements were conducted using either a Picarro analyzer or a Los Gatos ICOS Analyzer, with Stephen Springston (Brookhaven National Lab, srs.bnl.gov) serving as the principal investigator for all campaigns except TCAP, for which Rebecca Trojanowski (Brookhaven National Laboratory, rtrojanowski@bnl.gov) served as the principal investigator. The instruments were calibrated in the field.

2.2 NOAA/NASA Data

The database for the Fire Influence on Regional to Global Environments and Air Quality experiment (FIREX-AQ NOAA/NASA)[5] is accessible at `https://www-air.larc.nasa.gov/cgi-bin/ArcView/firexaq?DC8=1?DC8=1`. The SP2 BC measurements were conducted by J. P. Schwarz and J. M. Katich (NOAA ESRL Chemical Sciences Division, joshua.p.chwarz@noaa.gov), with an operational detection range of 90-550 nm assuming a void-free density of 1.8 g/cm^{-3}. Data were removed if total particle loadings caused deadtime bias greater than 20 percent. There was a 20% uncertainty when bypassing the dilution system and a 40% uncertainty when sampling behind it. The laser aerosol sizer was operated by Richard Moore, Elizabeth Wiggins, Edward Winstead, Claire Robinson, Lee Thornhill, and Kevin Sanchez (NASA Langley, richard.h.moore@nasa.gov). The CO measurements were made using the DACOM diode laser spectrometer by John Nowak, Joshua DiGangi, and Hannah Halliday with Glenn S. Diskin (NASA Langley, glenn.s.diskin@nasa.gov) as the principal investigator. The VOC Halocarbon/Hydrocarbon Grab Samples (GC/MS) were collected by Donald R. Blake (University of California Irvine, drblake@uci.edu). Additionally, the value-added Fire Flags product was produced by J. P. Schwarz (NOAA ESRL Chemical Sciences Division, joshua.p.chwarz@noaa.gov).

[a] *Earth and Environmental Sciences Division, Los Alamos National Laboratory, NM 87545.*
[b] *X Computational Physics Division, Los Alamos National Laboratory, NM 87545.*
[c] *University of California, Davis, CA 95616.*

2.3 NSF Data

Data from the Western Wildfire Experiment for Cloud Chemistry Aerosol Absorption and Nitrogen study (WE-CAN NSF)[6,7] are available in the data archive at (https://doi.org/10.26023/NJ5F-K29V-T800). The SP2 BC measurements were conducted by Ezra J.T. Levin (Colorado State University, elevin@atmos.colostate.edu)[8].

3 Partitioning Parameterization

We used the VBS-BAT model for gas-to-particle equilibrium partitioning[9] to generate random data for parameterization. Total organic vapor concentrations were calculated from CO concentrations using emission correlations observed in Indonesian peat moss[10]. The total organic vapors were used to scale the biomass-burning volatility distribution, which was validated in a chemical transport model study by Theodoritsi and Pandis[11].

We randomly sampled total organic aerosol loading, VOC loading (via CO concentration), temperature, and relative humidity (RH) using 10,000 uniform-random samples within the following parameter ranges: CO (0.001 to 10000 μg/m^3), primary OA (1 to 10000 μg/m^3), RH (0% to 98%), and temperature (200 to 350 K). The biomass burning volatility distribution was temperature-dependent and accounted for using the Clausius-Clapeyron approximation presented in[12].

From the random sampling results, we parameterized the fraction of the total semi-volatile vapors that condensed, i.e., the partitioning coefficient ξ_{VOC}. We fitted the partitioning coefficient to a polynomial with temperature (T, Kelvin) and RH (water activity, $a_w * 100\%$) using three and two degrees, respectively. The polynomial is

$$\xi_{VOC} = 5.0775 + -2.508a_w - 0.0273T - 0.3504a_w^2 + 0.02061a_wT + 3.763 * 10^{-05}T^2 - 0.006a_w^3 + 0.00149a_w^2T + -3.9449 * 10^{-05}a_wT^2. \quad (1)$$

We set ceiling and floor limits of $0 < \xi_{VOC} < 1$ in the software implementation.

4 Vapor Pressures

Table of vapor pressures[13] used in the partitioning calculations for the measured organic vapors.

Table 1 Vapor pressures calculated[13]

	p_{sat} $Log(atm.)$ **@250 K**	p_{sat} $Log(atm.)$ **@270 K**	p_{sat} $Log(atm.)$ **@290 K**
1-Nonene	-9.08E+00	-7.67E+00	-6.53E+00
n-Undecane	-4.62E+00	-3.77E+00	-3.07E+00
1,2,4-Trimethylbenzene	-4.33E+00	-3.51E+00	-2.84E+00
1,3,5-Trimethylbenzene	-4.32E+00	-3.51E+00	-2.84E+00
Limonene	-4.29E+00	-3.49E+00	-2.84E+00
α-Pinene	-4.24E+00	-3.45E+00	-2.80E+00
4-Ethyltoluene	-4.17E+00	-3.38E+00	-2.72E+00
3-Ethyltoluene	-4.17E+00	-3.38E+00	-2.72E+00
2-Ethyltoluene	-4.13E+00	-3.35E+00	-2.70E+00
β-Pinene	-4.07E+00	-3.30E+00	-2.67E+00
Camphene	-4.03E+00	-3.27E+00	-2.64E+00
n-Propylbenzene	-4.02E+00	-3.25E+00	-2.60E+00
n-Decane	-3.99E+00	-3.21E+00	-2.57E+00

Table 1 Vapor pressures calculated[13]

	$p_{sat}\ Log(atm.)$ **@250 K**	$p_{sat}\ Log(atm.)$ **@270 K**	$p_{sat}\ Log(atm.)$ **@290 K**
i-Propylbenzene	-3.97E+00	-3.21E+00	-2.57E+00
Tricyclene	-3.94E+00	-3.18E+00	-2.55E+00
Myrcene	-3.89E+00	-3.13E+00	-2.50E+00
1-Decene	-3.87E+00	-3.11E+00	-2.48E+00
Bromoform (CHBr3)	-3.62E+00	-2.90E+00	-2.30E+00
Benzofuran	-3.59E+00	-2.88E+00	-2.29E+00
m,p-Xylene	-3.56E+00	-2.84E+00	-2.24E+00
o-Xylene	-3.52E+00	-2.81E+00	-2.22E+00
Ethylbenzene	-3.42E+00	-2.72E+00	-2.13E+00
n-Nonane	-3.38E+00	-2.68E+00	-2.09E+00
Styrene	-3.28E+00	-2.60E+00	-2.03E+00
Ethynylbenzene	-3.20E+00	-2.52E+00	-1.95E+00
Tetrachloroethylene (C2Cl4)	-3.18E+00	-2.50E+00	-1.94E+00
Chlorobenzene	-3.15E+00	-2.49E+00	-1.93E+00
Dibromochloromethane (CHBr2Cl)	-2.98E+00	-2.32E+00	-1.78E+00
Toluene	-2.85E+00	-2.21E+00	-1.68E+00
n-Octane	-2.81E+00	-2.17E+00	-1.64E+00
1-Octene	-2.71E+00	-2.09E+00	-1.56E+00
2,3,4-Trimethylpentane	-2.63E+00	-2.03E+00	-1.53E+00
Methylcyclohexane	-2.61E+00	-2.00E+00	-1.50E+00
2,2,4-Trimethylpentane	-2.58E+00	-1.99E+00	-1.49E+00
Isopropanol	-2.55E+00	-1.90E+00	-1.36E+00
Propionitrile	-2.49E+00	-1.89E+00	-1.39E+00
Acrylonitrile	-2.40E+00	-1.81E+00	-1.32E+00
Trichloroethylene (C2HCl3)	-2.33E+00	-1.74E+00	-1.25E+00
Dibromochloromethane (CHBrCl2)	-2.30E+00	-1.72E+00	-1.24E+00
Carbon tetrachloride (CCl4)	-2.29E+00	-1.73E+00	-1.27E+00
n-Heptane	-2.26E+00	-1.69E+00	-1.20E+00
2-Methylhexane	-2.23E+00	-1.66E+00	-1.18E+00
3-Methylhexane	-2.23E+00	-1.66E+00	-1.18E+00
Cyclohexane	-2.20E+00	-1.64E+00	-1.18E+00
Benzene	-2.18E+00	-1.62E+00	-1.15E+00
1-Heptene	-2.17E+00	-1.61E+00	-1.13E+00
2,3-Dimethylpentane	-2.17E+00	-1.61E+00	-1.15E+00
Dibromomethane (CH2Br2)	-2.11E+00	-1.55E+00	-1.09E+00
Methylchloroform (CH3CCl3)	-2.06E+00	-1.52E+00	-1.06E+00
Methylcyclopentane	-2.01E+00	-1.47E+00	-1.02E+00
Trichlorotrifluoroethane (CFC-113)	-1.97E+00	-1.43E+00	-9.83E-01
Methyl ethyl ketone (MEK)	-1.96E+00	-1.41E+00	-9.49E-01
Methyl vinyl ketone (MVK)	-1.86E+00	-1.33E+00	-8.80E-01
Butanal	-1.86E+00	-1.32E+00	-8.65E-01
1-Butene	-1.86E+00	-1.32E+00	-8.65E-01
Isobutanal	-1.83E+00	-1.30E+00	-8.47E-01
n-Hexane	-1.74E+00	-1.22E+00	-7.89E-01
2-Methylpentane	-1.71E+00	-1.20E+00	-7.72E-01

Table 1 Vapor pressures calculated[13]

	$p_{sat}\ Log(atm.)$ **@250 K**	$p_{sat}\ Log(atm.)$ **@270 K**	$p_{sat}\ Log(atm.)$ **@290 K**
3-Methylpentane	-1.71E+00	-1.20E+00	-7.72E-01
2,3-Dimethylbutane	-1.67E+00	-1.17E+00	-7.48E-01
2-Methylfuran	-1.66E+00	-1.15E+00	-7.23E-01
1-Hexene	-1.66E+00	-1.15E+00	-7.26E-01
3-Methylfuran	-1.65E+00	-1.14E+00	-7.16E-01
3-Methyl-1-pentene and 4-Methyl-1-pentene	-1.63E+00	-1.13E+00	-7.09E-01
Cyclopentene	-1.62E+00	-1.13E+00	-7.13E-01
Cyclopentane	-1.62E+00	-1.13E+00	-7.13E-01
Chloroform (CHCl3)	-1.62E+00	-1.13E+00	-7.14E-01
2,2-Dimethylbutane	-1.61E+00	-1.12E+00	-7.03E-01
Methyl acetate	-1.60E+00	-1.08E+00	-6.42E-01
Dichlorodifluoromethane (CFC-11)	-1.52E+00	-1.04E+00	-6.44E-01
1,2-Dichloroethane	-1.40E+00	-9.15E-01	-5.06E-01
Acetone propanal	-1.35E+00	-8.64E-01	-4.56E-01
2-Pentene	-1.33E+00	-8.56E-01	-4.61E-01
HCFC-141b	-1.29E+00	-8.25E-01	-4.31E-01
1,3-Pentadiene	-1.28E+00	-8.07E-01	-4.11E-01
1-Butyn-3-yne	-1.28E+00	-8.07E-01	-4.11E-01
Acrolein	-1.27E+00	-7.92E-01	-3.95E-01
Methyl iodide (CH3I)	-1.27E+00	-8.03E-01	-4.15E-01
n-Pentane	-1.25E+00	-7.85E-01	-3.94E-01
Isopentane	-1.23E+00	-7.67E-01	-3.82E-01
2-Pentanone nitrate (2-PentONO2)	-1.22E+00	-7.61E-01	-3.73E-01
3-Pentanone nitrate (3-PentONO2)	-1.22E+00	-7.61E-01	-3.73E-01
1-Pentene	-1.17E+00	-7.18E-01	-3.36E-01
Dichlorotetrafluoroethane (CFC-114)	-1.17E+00	-7.18E-01	-3.37E-01
2-Methyl-2-butene	-1.16E+00	-7.09E-01	-3.31E-01
2-Methyl-1-butene	-1.16E+00	-7.09E-01	-3.31E-01
3-Methyl-1-butene	-1.15E+00	-7.02E-01	-3.25E-01
Isoprene	-1.12E+00	-6.68E-01	-2.85E-01
Furan	-1.05E+00	-6.13E-01	-2.43E-01
2-Butyne	-9.75E-01	-5.35E-01	-1.66E-01
Dichloromethane (CH2Cl2)	-9.12E-01	-4.81E-01	-1.19E-01
trans-2-Butene	-8.58E-01	-4.38E-01	-8.42E-02
trans-2-Pentene	-8.58E-01	-4.38E-01	-8.42E-02
cis-2-Butene	-8.58E-01	-4.38E-01	-8.42E-02
Dichlorodifluoromethane (CFC-12)	-7.94E-01	-3.85E-01	-4.15E-02
n-Butane	-7.82E-01	-3.67E-01	-1.79E-02
Isobutane	-7.64E-01	-3.55E-01	-1.08E-02
2-Butanone nitrate (2-ButONO2)	-7.56E-01	-3.46E-01	3.19E-04
Methyl bromide (CH3Br)	-7.28E-01	-3.21E-01	2.16E-02
Isobutene	-7.02E-01	-3.01E-01	3.64E-02
1,3-Butadiene	-6.65E-01	-2.56E-01	8.98E-02
Ethyl chloride (C2H5Cl)	-6.22E-01	-2.22E-01	1.15E-01

Table 1 Vapor pressures calculated[13]

	$p_{sat}\ Log(atm.)$ **@250 K**	$p_{sat}\ Log(atm.)$ **@270 K**	$p_{sat}\ Log(atm.)$ **@290 K**
1-Butyne	-5.99E-01	-1.97E-01	1.42E-01
HCFC-142b	-5.31E-01	-1.40E-01	1.90E-01
Propane	-3.38E-01	2.98E-02	3.40E-01
n-Propyl nitrate (nPropONO2)	-3.26E-01	4.19E-02	3.53E-01
Isopropyl nitrate (iPropONO2)	-3.15E-01	4.89E-02	3.56E-01
Propene	-2.73E-01	8.52E-02	3.88E-01
1,2-Butadiene	-2.71E-01	8.45E-02	3.85E-01
Methyl chloride (CH3Cl)	-1.87E-01	1.75E-01	4.80E-01
Propyne	-1.56E-01	1.98E-01	4.98E-01
HCFC-22	-1.47E-01	2.02E-01	4.98E-01
Dimethyl sulfide (DMS)	8.30E-02	4.04E-01	6.76E-01
Ethane	8.36E-02	4.07E-01	6.80E-01
Ethyl nitrate (EthONO2)	9.68E-02	4.21E-01	6.95E-01
HFC-134a (1,1,1,2-Tetrafluoroethane)	1.51E-01	4.66E-01	7.32E-01
HFC-152a (1,1-Difluoroethane)	1.92E-01	5.03E-01	7.66E-01
Propadiene (Allene)	2.75E-01	5.78E-01	8.35E-01
Ethene (Ethylene)	2.77E-01	5.83E-01	8.42E-01
Nitromethane	5.10E-01	7.99E-01	1.04E+00
Methyl nitrite (MeONO2)	5.10E-01	7.99E-01	1.04E+00
Ethyne (Acetylene)	6.07E-01	8.91E-01	1.13E+00
Carbonyl sulfide (OCS)	8.74E-01	1.11E+00	1.31E+00

5 Summary of Data Points for BC Mass Fraction Calculation

This section presents a summary for each campaign, highlighting the number of data points utilized in calculating the Black Carbon (BC) mass fraction, see Fig. 1. Notably, this summary excludes the PyroCb campaign data, as it did not conform to the automated in-smoke flag analysis. For PyroCb, a minimum of 10 data points were recorded per altitude bin.

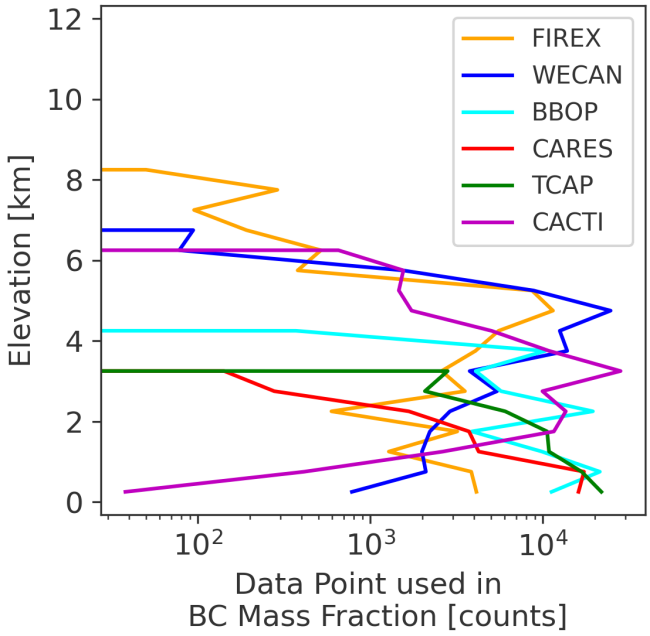

Figure 1 The figure illustrates the number of data points each campaign contributed towards the calculation of the median and percentiles for BC mass fraction. The PyroCb campaign data, not included in this automated in-smoke analysis, registered a minimum of 10 data points per altitude bin.

6 Additional Simulations

This section presents two supplementary LES experiments. Figure 2 illustrates the results of these simulations. The first simulation operates at a reduced wind speed of 1 m/s, while the second replicates the conditions described in the main manuscript. These simulations primarily investigate the dynamics of Organic Aerosol (OA) condensation.

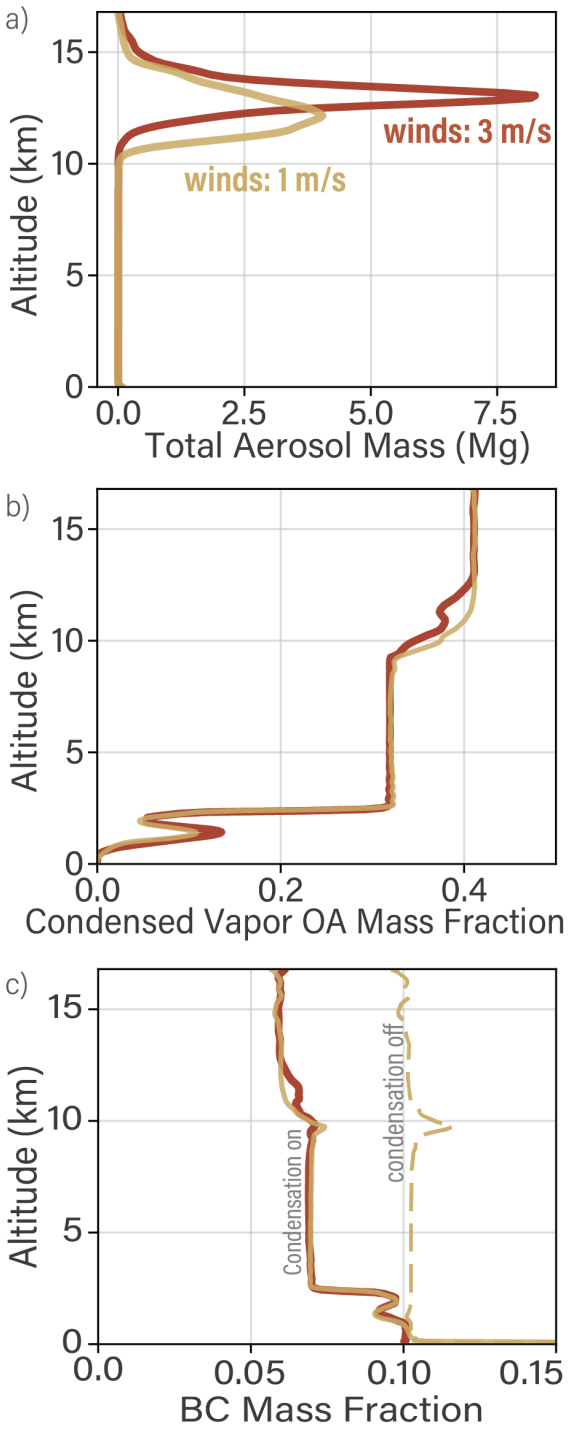

Figure 2 Altitude profiles from 12.5-hour LES runs are depicted, contrasting wind speeds of $1\ m/s$ (gold line) and $3\ m/s$ (red line). **(a)** Displays the altitude profile for total aerosol concentration. **(b)** Shows the condensed vapor fraction of the total OA, calculated as the ratio of vapor condensed to the sum of OA primary and vapor condensed. **(c)** Presents the BC mass fraction, comparing results from simulations with and without active organic vapor condensation.

References

[1] L. Kleinman and A. J. Sedlacek, *Biomass Burning Observation Project (BBOP) Final Campaign Report*, 2016.

[2] R. Zaveri, W. J. Shaw, D. J. Cziczo, B. Schmid, R. a. Ferrare, M. L. Alexander, M. Alexandrov, R. J. Alvarez, W. P. Arnott, D. B. Atkinson, S. Baidar, R. M. Banta, J. C. Barnard, J. Beranek, L. K. Berg, F. Brechtel, W. a. Brewer, J. F. Cahill, B. Cairns, C. D. Cappa, D. Chand, S. China, J. M. Comstock, M. K. Dubey, R. C. Easter, M. H. Erickson, J. D. Fast, C. Floerchinger, B. a. Flowers, E. Fortner, J. S. Gaffney, M. K. Gilles, K. Gorkowski, W. I. Gustafson, M. Gyawali, J. Hair, R. M. Hardesty, J. W. Harworth, S. Herndon, N. Hiranuma, C. Hostetler, J. M. Hubbe, J. T. Jayne, H. Jeong, B. T. Jobson, E. I. Kassianov, L. I. Kleinman, C. Kluzek, B. Knighton, K. R. Kolesar, C. Kuang, A. Kubátová, a. O. Langford, A. Laskin, N. Laulainen, R. D. Marchbanks, C. Mazzoleni, F. Mei, R. C. Moffet, D. Nelson, M. D. Obland, H. Oetjen, T. B. Onasch, I. Ortega, M. Ottaviani, M. Pekour, K. a. Prather, J. G. Radney, R. R. Rogers, S. P. Sandberg, A. Sedlacek, C. J. Senff, G. Senum, A. Setyan, J. E. Shilling, M. Shrivastava, C. Song, S. R. Springston, R. Subramanian, K. Suski, J. Tomlinson, R. Volkamer, H. W. Wallace, J. Wang, a. M. Weickmann, D. R. Worsnop, X.-Y. Yu, A. Zelenyuk and Q. Zhang, *Atmospheric Chemistry and Physics*, 2012, **12**, 7647–7687.

[3] D. Cziczo, *Understanding the Effect of Aerosol Properties on Cloud Droplet Formation during TCAP Field Campaign Report*, 2016.

[4] A. Varble, S. Nesbitt, P. Salio, E. Avila, P. Borque, P. DeMott, G. McFarquhar, S. van den Heever, E. Zipser, D. Gochis, R. Houze, M. Jensen, P. Kollias, S. Kreidenweis, R. Leung, K. Rasmussen, D. Romps and C. Williams, *Cloud, Aerosol, and Complex Terrain Interactions (CACTI) Field Campaign Report*, 2019.

[5] C. Warneke, J. P. Schwarz, J. Dibb, O. Kalashnikova, G. Frost, J. A. Saad, S. S. Brown, W. A. Brewer, A. Soja, F. C. Seidel, R. A. Washenfelder, E. B. Wiggins, R. H. Moore, B. E. Anderson, C. Jordan, T. I. Yacovitch, S. C. Herndon, S. Liu, T. Kuwayama, D. Jaffe, N. Johnston, V. Selimovic, R. Yokelson, D. M. Giles, B. N. Holben, P. Goloub, I. Popovici, M. Trainer, A. Kumar, R. B. Pierce, D. Fahey, J. Roberts, E. M. Gargulinski, D. A. Peterson, X. Ye, L. H. Thapa, P. E. Saide, C. H. Fite, C. D. Holmes, S. Wang, M. M. Coggon, Z. C. J. Decker, C. E. Stockwell, L. Xu, G. Gkatzelis, K. Aikin, B. Lefer, J. Kaspari, D. Griffin, L. Zeng, R. Weber, M. Hastings, J. Chai, G. M. Wolfe, T. F. Hanisco, J. Liao, P. C. Jost, H. Guo, J. L. Jimenez and J. Crawford, *Journal of Geophysical Research: Atmospheres*, 2023, **128**, 1, 62.

[6] E. Fisher, J. Collett, A. Sullivan, P. DeMoot, S. Murphy, J. Thornton, F. Flocke, S. van den Heever, D. Toohey and L. Hu, *Western Wildfire Experiment for Cloud Chemistry, Aerosol Absorption and Nitrogen*, 2017.

[7] E. NASA/NOAA, *WE-CAN: Low Rate (LRT - 1 sps) Navigation, State Parameter, and Microphysics Flight-Level Data. Version 1.1 (Version 1.1) [Data set].*, 2023.

[8] E. Levin, *Single Particle Soot Photometer (SP2) Black Carbon Mass in Individual Particles Data.*, 2019.

[9] K. Gorkowski, T. C. Preston and A. Zuend, *Atmospheric Chemistry and Physics*, 2019, **19**, 13383–13407.

[10] L. E. Hatch, R. J. Yokelson, C. E. Stockwell, P. R. Veres, I. J. Simpson, D. R. Blake, J. J. Orlando and K. C. Barsanti, *Atmospheric Chemistry and Physics*, 2017, **17**, 1471–1489.

[11] G. N. Theodoritsi and S. N. Pandis, *Atmospheric Chemistry and Physics*, 2019, **19**, 5403–5415.

[12] N. M. Donahue, J. H. Kroll, S. N. Pandis and A. L. Robinson, *Atmospheric Chemistry and Physics*, 2012, **12**, 615–634.

[13] S. Compernolle, K. Ceulemans and J.-F. Müller, *Atmospheric Chemistry and Physics*, 2011, **11**, 9431–9450.